

Evolutionary computation for adaptive quantum device design

Luke Mortimer,¹ Marta P. Estarellas,² Timothy P. Spiller,¹ and Irene D'Amico¹

¹*Department of Physics, University of York, York, YO10 5DD, United Kingdom*

²*National Institute of Informatics, 2-1-2 Hitotsubashi, Chiyoda-ku, Tokyo 101-8430, Japan*

As Noisy Intermediate-Scale Quantum (NISQ) devices grow in number of qubits, determining good or even adequate parameter configurations for a given application, or for device calibration, becomes a cumbersome task. We present here an evolutionary algorithm that allows for the automatic tuning of the parameters of a spin network (an arrangement of coupled qubits) for a given task. We exemplify the use of this algorithm with the design schemes for two quantum devices: a quantum wire and a multi-qubit gate. The designs obtained by our algorithm exploit the natural dynamics of the system and perform such tasks with fidelities of 99.7% for the state transfer through a quantum wire and 99.8% for the application of a controlled-phase gate. Such designs were previously unknown, with this wire scheme able to transfer quantum information with high fidelity in a shorter time than previous spin chain designs of the same length. With such encouraging results, our approach has the potential to become a powerful technique in the design and calibration of NISQ devices.

I. INTRODUCTION

Quantum technologies have already extensively advertised their potential to impact a wide spectrum of fields. The first proof-of-principle demonstrations of quantum advantage in terms of computational power, also known as *quantum supremacy* [1], have already been achieved [2], satellite-based quantum protected key sharing (quantum key distribution, QKD) has been realized [3] and early prototypes of a first quantum internet are starting to be devised [4]. Nevertheless, the application range is so varied that there is no established preferred physical implementation of the hardware for such early devices and an hybridized approach of the technology is currently being undertaken [5].

The excellent controllability of superconducting qubits and ion traps makes them good candidates to build early models of quantum chips at the NISQ (Noisy Intermediate-Scale Quantum) level [6–8]. Spin qubit systems, such as NV-centers, with their long coherence times have potential advantages for quantum sensing and memory applications [9–11], whilst photonic systems are preferred when it comes to long-range communication through either free space [12, 13] or optical fibre [14, 15]. With quantum devices being so diverse and heterogeneous, spin networks become a convenient mathematical model able to capture the quantum dynamics of any arrangement of two-level quantum systems coupled to each other independent of the actual physical implementation [16]. The specificity of each physical system is instead captured by the network topology and the energy scale of its parameters.

The simulation of quantum chips under the spin network formalism proves to be a useful test-bed for the study and design of new quantum hardware and its applications. Such systems are very versatile and have been en-

gineered for different purposes, e.g. to allow for perfect state transfer (PST) [17–21], to present topologically protected states [22–24] or to act as quantum gates [25–31], amongst others. However, to achieve the desired dynamical behavior the ability is required to tune or calibrate the system parameters (such as the interaction energies, or *couplings*, between the different nodes or qubits of the network), as well as choosing a suitable network topology.

Whilst available technology already allows for an excellent controllability of such parameters in the laboratory [2], finding suitable tuning as well as an appropriate network topology in the design of quantum devices is a non-trivial task for complex systems beyond toy-models. The number of possibilities and combinations is so vast that determining good or even adequate solutions for a given task can be not only cumbersome, but also counter-intuitive. To circumvent this, here we propose to use tools common in evolutionary computation [32] for the design of quantum devices via the engineering of spin networks. This computational paradigm was originally proposed in the 1970s with the idea of using concepts of natural evolution to solve hard computational tasks in optimization, design and modelling [33]. Since then, this model of computation has proven to be a powerful tool for problems that do not necessarily require optimal solutions, but instead can utilise appropriate approximations to these.

Within this field, genetic algorithms are the most popular techniques and these have widely been applied to solve large engineering problems, ranging from antenna design [34] and complex aerodynamic modelling [35], to the improvement of artificial neural networks [36] and the automatic identification of analytical equations underlying physics phenomena [37]. The design of such systems is characterized by the number and complexity of its degrees of freedom, something that makes the number of possible configurations exponentially large. Genetic algo-

gorithms are highly parallelizable meta-heuristic optimization techniques able to efficiently cover such large search spaces and thus find approximate solutions [38]. Quantum systems presents similarities to these problems in terms of complexity, making genetic methods promising candidates to automate the search of appropriate design solutions.

In order to show this, we propose here a genetic algorithm capable of identifying optimal tuning parameters of a spin network to achieve a given task. Even though our algorithm is general and could be applied to any given problem of this sort, to exemplify its use we here focus on two tasks: the engineering of quantum devices for quantum state transfer and the design of multi-qubit gates. We demonstrate that the proposed automated technique has the potential of finding new system configurations that were previously unknown. While machine learning algorithms have recently been proved useful for quantum device tuning [39, 40], we demonstrate that evolutionary algorithms are also promising candidates for the general control and calibration of quantum chips, a technological challenge in NISQ-based computation. Altogether, our results show that only a minimal number of iterations is required to optimise the network parameters for most tasks.

II. SPIN CHAIN MODEL

We consider a general spin network of N sites (also referred to as spins, nodes or qubits) that can be described by the following time-independent XXZ-Heisenberg Hamiltonian:

$$\hat{H} = \sum_{i < j} J_{ij} \left(|1\rangle \langle 0|_i \otimes |0\rangle \langle 1|_j + h.c. \right) + \sum_{i=1}^N \epsilon_i |1\rangle \langle 1|_i + \sum_{i < j} \alpha J_{ij} \left(|1\rangle \langle 1|_i \otimes |1\rangle \langle 1|_j \right) \quad (1)$$

with J_{ij} being the real-valued coupling between sites i and j and ϵ_i the on-site energies (uniform and scaled to zero unless stated otherwise). In our encoding, we consider the injection of an excitation to be the creation of a spin “up”, $|1\rangle$, in a system that has initially been prepared to have all the spins “down”, $|0\rangle$.

The interaction term is proportional to the constant dimensionless scaling factor α . For $\alpha \neq 0$, this term represents the interaction energy between two excitations [41] and thus affects the dynamics of subspaces containing at least two excitations. The topology of the network is de-

finied by the non-zero elements of J_{ij} , the values of which are the target of our optimisation. Throughout this paper, J_{\max} indicates the maximum value of the couplings for a given system.

Once the parameters are set, we obtain the eigenvectors and eigenvalues of the Hamiltonian matrix by direct diagonalisation. Then any chosen initial state is decomposed into the eigenvectors, which are each evolved via the unitary operator $U = e^{-\frac{i}{\hbar} E_i t}$, with E_i being the corresponding eigenvalue. This allows us to obtain the overall state of the system at any time with the same accuracy.

We use the fidelity as a measure to assess how close the state of the system at a given time $|\Psi(t)\rangle$ is to the specific target state $|\Psi_{\text{target}}\rangle$ required for our task. The fidelity $F(t)$ ranges between zero and unity, with maximum fidelity representing a perfect overlap between target and actual state:

$$F(t) = |\langle \Psi_{\text{target}} | \Psi(t) \rangle|^2. \quad (2)$$

III. GENETIC ALGORITHM

General genetic algorithms rely on the evaluation of different parametrizations of a system’s degrees of freedom to perform a given task. This evaluation is done through the calculation of a “fitness” score, which indicates how close a given parametrization is to optimality. In our implementation, the parameters to be tuned are the set of non-zero coupling energies of Eq. 1.

The flowchart in Fig. 1 shows a schematic of the route followed by our genetic algorithm. The first and most critical step to design a genetic algorithm is to define a proper structure of what is called the “genome”. As in DNA, the genome is represented as a string containing the mutable information of a system; this is, its degrees of freedom. The algorithm starts with a set of different genomes being evaluated according to a fitness function. After this evaluation, the better genomes are favoured to combine (‘crossover’) with other successful genomes, based on their fitness scores, to form the next generation. After crossing-over two genomes, a random modification is then made to the resulting genome to allow for new and unique solutions to be found [42].

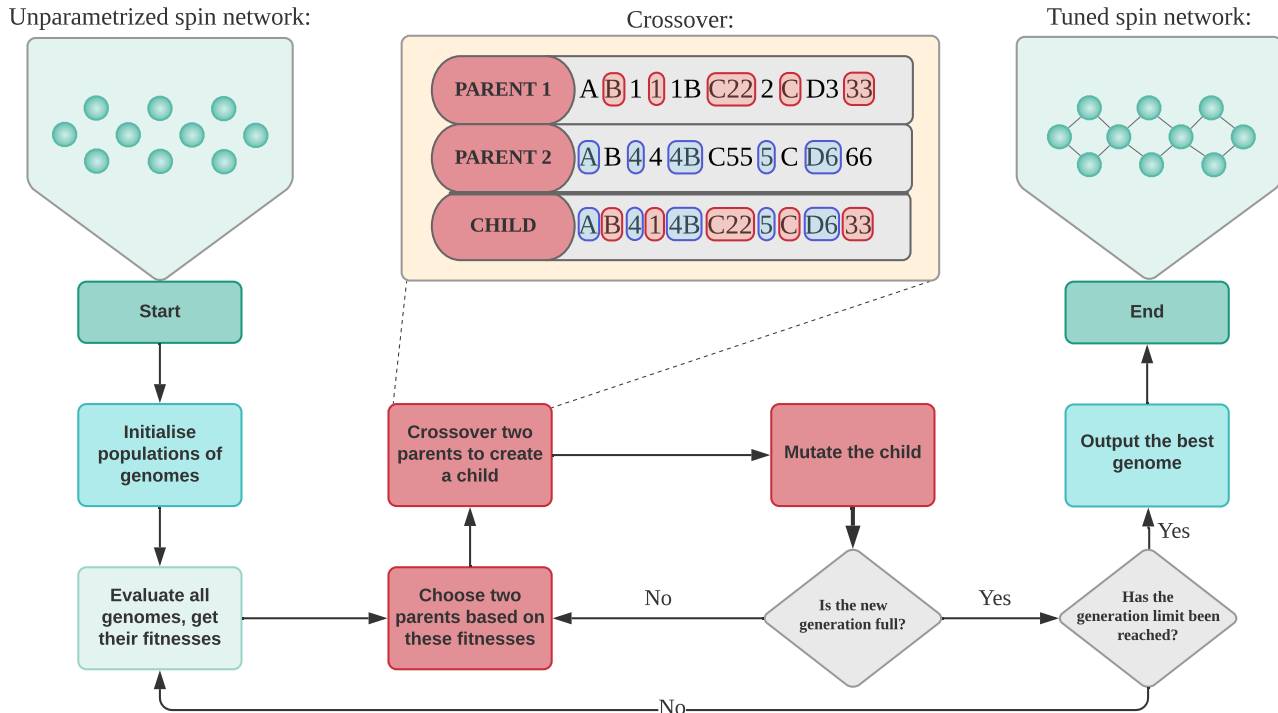


FIG. 1: Flowchart showing a schematic representation of our genetic algorithm. In the central panel we present a diagram displaying the method used to crossover two genomes. For each character in the child genome, the corresponding character from one of the parents is used, with each having equal probability.

A. A Genome For a Spin Network

In order to properly utilise the features of a genetic algorithm, it is important to find an effective representation of the spin network in a standardised notation, so that it can be easily passed as an argument to the various functions of the program. As such, it should contain all of the system's relevant information, whilst also being easy to store, modify and transfer. The genome we chose to use here is represented as a fixed-size linear string of standard ASCII characters, split into various sections representing information useful for the different functions. There also exist some optional features that can be added into the string to specify more unique requirements.

In our genome, letters are used to represent the sites and their corresponding single-excitation basis vectors, whilst couplings energies are represented as integers. For example, $AB500$ would represent a coupling strength of 500 between sites A and B of a spin network, relative to any other specified couplings. A bra-ket $\langle \dots | \dots \rangle$ at the start specifies the initial and target states of the system's protocol, which is the information necessary to evaluate the performance of such a genome through its

fidelity (Eq. 2). In this bra-ket, two letters placed adjacent are treated as the tensor product of the two single excitation basis vectors, for instance $\langle AB | = \langle 11 |_{AB}$, thus allowing the use of multiple excitation subspaces. Superpositions can be described through addition, with an optional phase $(-1, i, (1 + 2i), \text{etc.})$, such that $|A + iB\rangle = \frac{1}{\sqrt{2}}(|10\rangle_{AB} + i|01\rangle_{AB})$. Note that in the algorithm all state vectors are automatically normalised, so normalization factors are left out from the genome.

Two simple genomes representing a 3- and a 4-spin network are given in Fig. 2, (a) and (b) respectively. In Fig. 2a), an initial excitation is injected at site A, $|\Psi(0)\rangle = |100\rangle_{ABC}$, and then, at each time within a chosen set, the fidelity is evaluated against the target state $|\Psi_{\text{target}}\rangle = |001\rangle_{ABC}$. This genome specifies two coupling energies with relative values of 500 (between A and B) and 500 (between B and C), thus representing a uniform chain.

In Fig. 2b), a more complicated example is presented. This genome represents a small spin network able to generate an entangled state between sites C and D, $|\Psi_{\text{target}}\rangle = |00\rangle_{AB} \otimes \frac{1}{\sqrt{2}}(|10\rangle_{CD} + |01\rangle_{CD})$, when a single excitation is injected at site A, $|\Psi(0)\rangle = |1000\rangle_{ABCD}$.

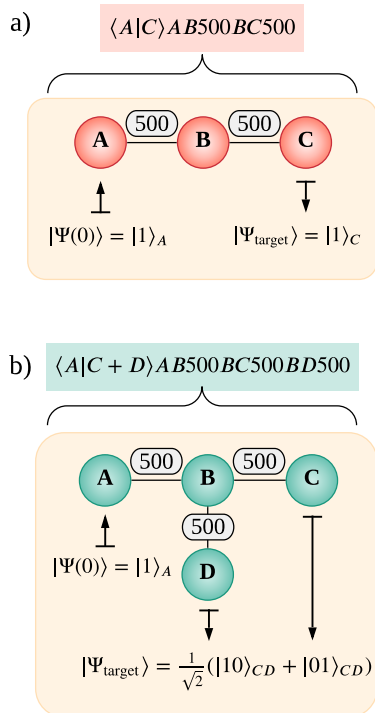


FIG. 2: Examples of the construction of a genome in our algorithm. **a)** Uniformly coupled ($J = 500$) $N=3$ spin chain with initial state $|\Psi(0)\rangle = |100\rangle_{ABC}$ and target state $|\Psi_{\text{target}}\rangle = |001\rangle_{ABC}$. **b)** Uniformly coupled ($J = 500$) spin network with initial state $|\Psi(0)\rangle = |1000\rangle_{ABCD}$ and target state $|\Psi_{\text{target}}\rangle = |00\rangle_{AB} \otimes \frac{1}{\sqrt{2}}(|10\rangle_{CD} + |01\rangle_{CD})$. Note that in the diagram factorizable $|0\rangle$ states are left out for convenience.

There are also some more niche genome features. A target time can be specified anywhere in the genome with syntax '@12.40' to force the algorithm to optimise the dynamics of the system to reach the target state at, for instance, $t_f = 12.40/J_{\text{max}}$. This substantially increases the speed of the algorithm since only a single-point calculation corresponding to that specific time point is required, rather than evaluating the full dynamics (and searching) over a time window. Although this allows for faster optimisation, it removes any flexibility in the time and thus should only be used if the transfer time is known, or is to be specified rather than allowed to vary. As such, it is often useful to perform a short optimisation without this feature first, to see the time that the system naturally evolves towards, and then perform a subsequent optimisation specific to that time.

Non-uniform on-site energies can also be specified, achieved by including a repeated-letter coupling (such as AA650). Negative couplings are also allowed, which could be of interest when evaluating systems of different magnetic order, such as anti-ferromagnetic lattices [43].

These are achieved through specifying a coupling with the letters in reverse-alphabetical order, such that BA500 represents -500 . Such notation is used to keep genome length constant and concise. There also exists optional notation related to the visualisation of the genome [44].

B. Fitness

For the evaluation of the genomes one needs to define first a fitness function which takes a genome string as an input and returns its fitness (normalised to be a number between 0 and 100), indicating how well such a genome satisfies the protocol or device requirements. This function combines various factors such as the maximum fidelity between the evolving state and the target state, along with the time at which that state is reached, all scaled by customisable parameters. The function is also chosen to be exponential in order to give any genome which is mutated positively a more significant boost in fitness, allowing it a higher chance of continuation. The overall equation for this function is given as

$$f(F_{\text{max}}, t_f) = 100 \exp(a(1 - F_{\text{max}})) \exp(bt_f J_{\text{max}}), \quad (3)$$

where F_{max} is the maximum fidelity, t_f is the time, in units of $1/J_{\text{max}}$, to reach F_{max} . a and b are arbitrary scaling factors, by default 10 and -0.001 , respectively. The maximum fidelity is found by searching the dynamics of the system over a search window, by default between 0 and $20/J_{\text{max}}$ divided into 100 increments (for a balance of search resolution and performance).

A fitness score of 100 for a spin-chain designed as a state-transfer device would thus mean that the transfer has been unrealistically achieved with zero waiting time ($t_f = 0$) and perfect fidelity ($F(t_f) = 1$), whilst a value approaching 0 would suggest either no information transfer at all or that it takes so long in time that it is not an effective solution. This fitness is then used to determine the likelihood that the features contained within a certain genome will continue through the generations.

C. Crossover and Mutation

In order to create the next generation, genomes from the previous generation are selected with a probability proportional to their fitness score. When two genomes are selected, they are combined in a process known as crossover. In this particular implementation, crossover involves iterating over the number of characters in the

parent genomes and for each genome position randomly choosing (with equal probability) one of the parents from which to take the character, as shown visually in the crossover panel of Fig. 1. Note that since both genomes share the same letter order, it is only the coupling values which change.

This new genome, also referred to as the child, is then “mutated” by increasing or decreasing one of its couplings by a random integer less than or equal to the maximum mutation size, μ , generated uniformly. The new coupling is capped between 0 and the highest possible coupling for that genome, unless negative couplings are explicitly allowed. This μ begins at some initial value, μ_i , and is linearly decreased to some specified final value, μ_f , as the generations continue to allow the algorithm to make more specific changes after initially covering a very wide search space. μ_i is by default 20% of the maximum possible coupling, such that for a 3 digit genome each mutation could initially change by up to 20% of 999: meaning $\mu_i = 200$. However, this should be changed to be higher or lower if a system requires more or less extreme changes, respectively. μ_f is set to one by default, but should also be increased if μ should remain higher throughout the optimisation. New genomes are generated in this manner until an entirely new generation is created to replace the old one.

The overall process then repeats for a large number of generations, with each iteration resulting in an increased average fitness score until either a target fitness is reached or the program reaches some maximum elapsed iteration.

D. Parallelisation and Scaling

A useful property of genetic algorithms is that they can be highly parallelized. In our case, we have been able to efficiently parallelize our algorithm using a standard implementation of the Message Passing Interface (MPI). This allowed large networks with multiple excitations to be fully optimised within an hour, which otherwise would have taken a day. This is all done by distributing the evaluation of each generation between the CPU cores, providing near embarrassingly parallel speedup.

The parallel performance of the code is shown in Fig. 3, which shows how the time taken to optimise a system is reduced by a factor of approximately two using two cores, four with four cores etc., a concept known as parallel speedup, ideally an identity function. The optimisations used for this test are ran for a fixed number of generations (here 200) to focus more on the efficiency of the algorithm than on the ease of optimising each given system. A positive feature is that the scaling is better for larger systems, since more time is spent evaluating each

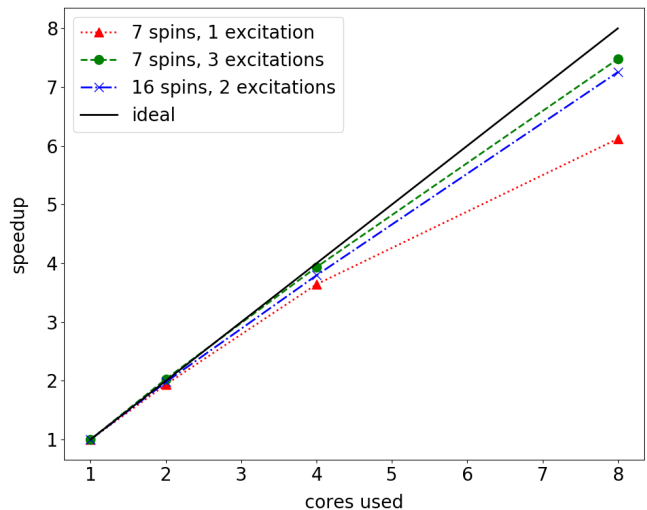


FIG. 3: Plot showing how the software scales for a given system as the number of CPU cores used in parallel is increased. Three systems are used for demonstration: a linear chain of 7 sites using a single excitation, the same chain but with three excitations, and a 16 spin grid with two excitations. Each is optimised using 1024 genomes for 200 generations. Each run was repeated 5 times to improve timing consistency. Note how scaling becomes closer to the ideal case as the subspaces become larger, allowing more efficient CPU usage.

genome, done entirely in parallel, compared to smaller systems in which most of the time is spent on the more trivial serial operations, such as distributing/collecting the genomes between cores. Discussion of the scaling with respect to the excitation-subspace is also given in the supplementary material [44].

IV. EXAMPLES

We now provide examples of the application of the aforementioned algorithm for the design of different devices, using modest-size spin networks. Each of these is required to act either as a quantum wire or a quantum gate.

A. Design of a Quantum Wire

As with classical computers and conventional data, a quantum computer processor requires quantum wires to be able to transmit quantum data between registers. Clearly the use of photonics for such short range communication presents some drawbacks: quantum computer

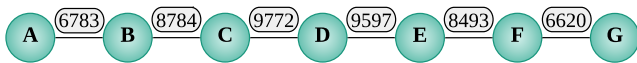


FIG. 4: A linear chain of seven spins optimised for both speed and PST. This maps $|1\rangle_A$ to $|1\rangle_G$ at time $t_f = 5.40/J_{\max}$ with 99.7% fidelity.

hardware is generally built out of static matter qubits (e.g. superconductors, ion traps or quantum dots) and the use of photons would imply the conversion of the matter qubit state into states of light and vice-versa, a costly process for such short distances. Instead, Bose pioneered the idea of using spin chains as quantum data buses [45, 46], an idea that attracted significant interest and was soon investigated by many [17, 47, 48]. One of the motivations for doing this was the possibility of building a wire with the same type of solid-state qubit as the rest of the hardware, to avoid conversion between different forms of qubit.

The use of chains of matter qubits as data buses requires a method to transport an arbitrary quantum state from one site to another, possibly through the natural dynamics of the system (and therefore with little external control). Such quantum state transfer can be enabled with high fidelity through many strategies [20, 49–51], one of the most popular ways being the engineering of the spin-spin interactions of a one-dimensional chain.

As these are simple and well-understood systems, in order to test our genetic approach we first check whether or not our algorithm can effectively identify some of the known coupling patterns that enable a spin chain to act as a wire. Our initial configuration is a linear chain of seven spins and we consider the transfer of an excitation being injected at the first or input site (site A in Fig. 4) to its mirror position or output site (here, site G). The quality of the transfer is therefore assessed by calculating the fidelity between the evolved state, $|\Psi(t)\rangle$, and the target state of an excitation appearing only at the output site. The transfer is perfect when this fidelity is one.

The algorithm begins with a generation of genomes all with uniform couplings, then within only a few new generations (see Fig. 5) the genomes converge close to one of the most well-known coupling configurations for PST [17, 18]. Here the $N - 1$ interactions of an N -site linear chain are defined as,

$$J_{i,i+1} = J_0 \sqrt{i(N-i)}, \quad (4)$$

with i being the site number and J_0 a constant that sets the energy scale. The resultant structure is presented in Fig. 4. We note that as this example utilises only the one-

excitation subspace, the last term in the Hamiltonian (1) does not contribute, regardless of the value of α .

The couplings of the ideal PST chain from Eq. 4 and those obtained from the algorithm are compared in Fig. 5. Due to the fitness function also having a dependence on speed, the optimized couplings were slightly closer to uniform than those given by Eq. 4, as shown in Fig. 5, resulting in a slightly faster transfer at the expense of a small amount of fidelity: $t_f = 5.4/J_{\max}$ with 99.7% fidelity vs $t_f = 5.44/J_{\max}$ with 100% fidelity.

Changing the parameters of the fitness function would result in a different result being converged upon, allowing flexibility depending on the physical application, e.g. taking into account factors like the decoherence time and ability to apply error-correction techniques. For instance, in this example, an emphasis on shorter t_f could be included by changing the value of b (from Eq. 3): the same optimisation with b set to -1000 results in a transfer time of $4.8/J_{\max}$, at a fidelity of 92.6%.

The best, average and worst fitness scores for each generation during this optimisation are displayed in Fig 6, which shows how few generations are required for this method to reach a high fitness score for such simple systems. Note that here the optimisation was stopped after the default maximum number of generations (200) as a demonstration, but could have been stopped much sooner and still retained fast and high fidelity transfer. Corresponding graphs for the optimisation of other systems are given in the supplementary material [44]. Importantly, although a simple method could be to take only the best genomes for each generation, the best fitness may then become trapped at a local maximum, whilst worse solutions may eventually reach a higher fitness if allowed to evolve down their path.

With the previous example being a toy-model test, we now move to optimise more complex, non-trivial networks for PST, for which our algorithm becomes more interesting. Here a simple “shoelace” network was chosen as an example topology, initialized uniformly. When optimised as a quantum wire, it resulted in a transfer time of $t_f = 3.8/J_{\max}$ with 99.70% fidelity, with the resultant structure shown in Fig. 7. This is 32% faster than the equivalent 7-site PST linear chain described above, and is attained by simply adding two extra nodes that modify the topology away from a simple chain. The identification of faster structures highlights the potential for this method to create improved spin-channels between quantum computing components.

Initial	Final	4 s.f.	3 s.f.	2 s.f.	1 s.f.
$ 01\rangle_{RA}$	$ 01\rangle_{SF}$	99.8%	99.9%	99.8%	89.0%
$ 10\rangle_{RA}$	$ 10\rangle_{SF}$	99.9%	99.9%	99.9%	91.9%
$ 11\rangle_{RA}$	$- 11\rangle_{SF}$	99.8%	99.8%	99.6%	83.8%
$\frac{1}{2}(00\rangle_{RA} + 01\rangle_{RA} + 10\rangle_{RA} + 11\rangle_{RA})$	$\frac{1}{2}(00\rangle_{SF} + 01\rangle_{SF} + 10\rangle_{SF} - 11\rangle_{SF})$	99.8%	99.8%	99.8%	89.0%

TABLE I: Truth table showing the fidelities when the controlled phase gate genome is evaluated with different input injections and with various levels of genome precision, given as the number of significant figures (s.f.) used per coupling. Note that all sites are assumed to have no excitation unless otherwise specified (such that $|0\rangle$ states of non-relevant sites are omitted for clarity). The system is tailored so that each of these outputs is achieved at the same time of $12.4/J_{\max}$.

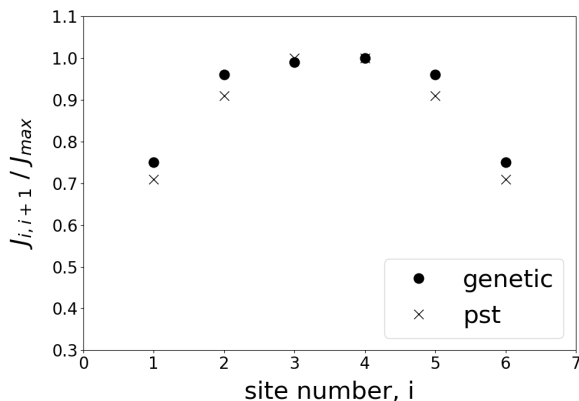


FIG. 5: Comparison for a $N = 7$ linear chain between the known couplings giving PST from Eq. 4 and the couplings converged upon by the algorithm with default settings. The distribution of generated couplings is flatter than those from Eq. 4 in order to increase speed somewhat at the expense of a small amount of fidelity. Both sets of values are scaled such that their maximum is one.

B. Design of a Quantum Gate

Whilst transferring quantum information quickly and reliably is one of the most popular uses of spin networks, when it comes to designing quantum hardware there may be situations where it would significantly aid computation if a quantum gate could be applied to the information being transferred. To do this with large spin networks one would need to find suitable tuning of the numerous parameters, something which would be difficult to achieve analytically. We thus identify such an example as one of the most appropriate use cases for our proposed method.

In the following test we start the design process with a 4×4 grid of spins plus two input and two output spins, with

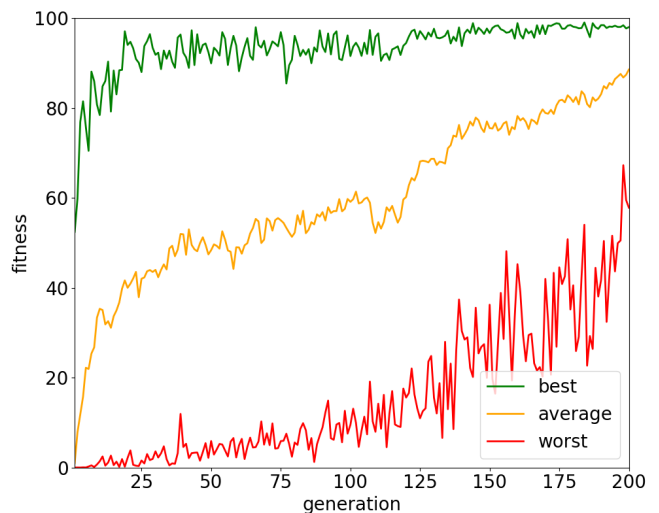


FIG. 6: Plot of the worst, average and best fitness scores for each generation when optimising a seven-site linear chain for PST. The size of mutations is reduced each generation, resulting in smaller, more precise, changes in fitness. This is the case except for the worst case scenario, where sometimes even small changes in the couplings results in large changes to fitness, which represents how the parameter space is being explored.

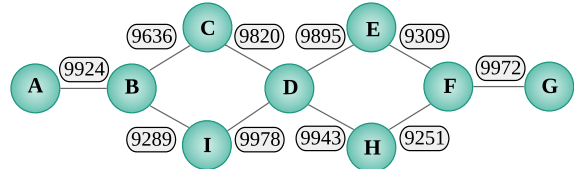


FIG. 7: A network of spins arranged in a shoelace pattern optimised for speed and PST. This maps $|1\rangle_A$ to $|1\rangle_G$ at time $t_f = 3.8/J_{\max}$ with 99.7% fidelity.

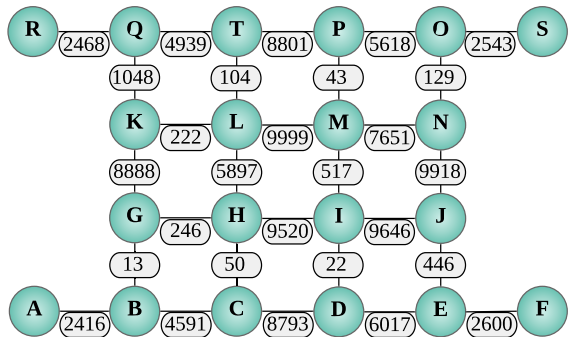


FIG. 8: A network optimised to perform a controlled phase gate on the two qubits, and mapping the state $\frac{1}{2}(|00\rangle_{RA} + |10\rangle_{RA} + |01\rangle_{RA} + |11\rangle_{RA})$ to $\frac{1}{2}(|00\rangle_{SF} + |10\rangle_{SF} + |01\rangle_{SF} - |11\rangle_{SF})$ with 99.8% fidelity at time $t_f = 12.40/J_{\max}$.

the aim of engineering the system to perform a controlled-Z gate on two qubits (see Table I). In Fig. 8 we draw the topology along with the optimized couplings: the gate is to be applied between qubits R and A, with the result being output at sites S and F.

The genetic algorithm was capable of identifying the tuning outlined in Fig. 8 with the device able to perform a controlled-Z gate, allowing for the initial state

$$|\Psi(0)\rangle = \frac{1}{2}(|00\rangle_{RA} + |01\rangle_{RA} + |10\rangle_{RA} + |11\rangle_{RA}),$$

to be mapped to the approximate final state of

$$|\Psi(t_f)\rangle \approx \frac{1}{2}(|00\rangle_{SF} + |01\rangle_{SF} + |10\rangle_{SF} - |11\rangle_{SF})$$

with 99.8% fidelity and a transfer time of $t_f = 12.40/J_{\max}$.

Importantly, this network is shown to retain the high $\approx 99.8\%$ fidelity even as the number of digits used in the genome is approximated from 4 to 3 and even 2 significant figures (s.f.), which would allow tolerance when implementing such a network physically, as shown in Table I. The approximation is done such that, for example, the 2 s.f. couplings are the 4 s.f. couplings, but rounded to the nearest 100 and then divided by 100 (e.g. $23 \rightarrow 0$, $2524 \rightarrow 25$ etc.). The fidelity for the genome with these 2 s.f. couplings is then evaluated and reported in Table I. This high tolerance would also suggest that to improve the performance of this particular network a change in

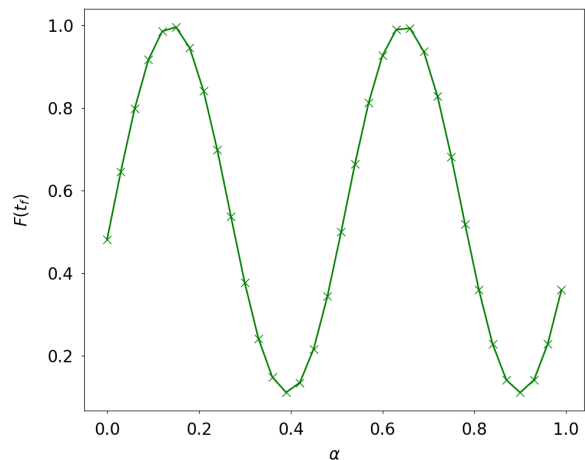


FIG. 9: Fidelity of the phase-gate vs α . The fidelity shows sinusoidal behaviour with respect to α . The first peak is reached at $\alpha = 0.141$ with a fidelity of 99.8%.

the topology is needed, rather than simply increasing precision of the genome.

In this example, unlike the others, the two-excitation coupling term in Eq. 1 affects the results when $\alpha \neq 0$. This term helps to build a phase specific to subspaces containing at least two excitations, allowing the network for the controlled phase gate to be optimised to reach higher fidelities. Without such a term, this topology was able to reach at most 77% fidelity, whilst optimising with $\alpha = 0.141$ allowed for the 99.8% fidelity result. In some physical implementations, this coupling term would correspond to a dipole-dipole interaction. A scaling factor of $\alpha = 0.141$ with respect to each coupling J_{ij} is then consistent with this second-order type of interaction.

Fig. 9 shows how the fidelity is affected when the phase-gate coupling scheme is evaluated using different values of α . It shows that the gate design is robust against small variation of α about its best value. The fidelity describes a sinusoidal with respect to the variation with α confirming that this term is responsible for the creation of a phase, and hence offering multiple choices of α for achieving best fidelity.

V. CONCLUSIONS

As quantum devices improve in terms of number of qubits and connectivity, the power of quantum computation gets an exponential boost. This however comes with the challenge that an increased number of degrees of freedom brings to the tuning of parameters when engineering quantum devices. To overcome this, we propose a novel method based on evolutionary computation that is capa-

ble of finding appropriate solutions from within the large search space of possible parametrizations. This method exploits a genetic algorithm that we have specifically designed to optimize the different degrees of freedom of a spin network to perform a given quantum information task. We provide examples showing the network structures discovered by the algorithm, one able to act as a controlled phase gate on two qubits and the others allowing for fast and high fidelity quantum information transfer.

In our examples we show that this method not only provides versatile candidates to connect quantum components with excellent transfer fidelities, but also allows for the design of quantum gates that exploit the natural dynamics of the spin system. Our genetic algorithm is capable of converging towards a parameter set that defines the connectivity of the network with coupling energies tailored to a customisable number of significant figures relative to each other. To this effect, we have also shown that high fidelities can be maintained for a network performing a controlled phase gate even when the number of significant figures in the couplings is reduced to just two. The stability of the fidelity against reducing the number of digits defining the coupling energies can be used as a test to understand the limits of a certain topology with respect to the desired application and can be used to identify implementations that are robust to experimental errors or control limitations.

It is important to note that our method allows optimisation with a tailored fitness function as well as the inclusion of a set of optional and flexible parameters. This versatility provides the possibility of a variety of use cases depending on the specific experimental constraints. For example, when designing a quantum state transfer device it may be preferable to transfer information faster at the expense of a lower fidelity in cases where decoherence times are relatively short. Our algorithm can be programmed with such constraints, making our method a promising candidate to assist in the design and calibration of real NISQ devices.

The method we proposed could be easily extended to include additional terms in the Hamiltonian, or to different model Hamiltonians. Future research would involve testing the method against a larger set of initial topologies for different quantum information tasks, such as additional gates. Another interesting point for further investigations would be extending this method to provide results bound by the experimental constraints of a specific quantum chip implementation.

VI. ACKNOWLEDGMENTS

M.P.E would like to acknowledge support from the Japanese MEXT Quantum Leap Flagship Program (MEXT Q-LEAP) Grant Number JPMXS0118069605. This project was in part undertaken on the Viking Cluster, a high performance computing facility provided by the University of York. We are grateful for computational support from the University of York High Performance Computing service, Viking and the Research Computing team.

-
- [1] John Preskill. Quantum computing and the entanglement frontier, 2012.
- [2] Frank Arute, Kunal Arya, Ryan Babbush, Dave Bacon, Joseph C Bardin, Rami Barends, Rupak Biswas, Sergio Boixo, Fernando GSL Brandao, David A Buell, et al. Quantum supremacy using a programmable superconducting processor. *Nature*, 574(7779):505–510, 2019.
- [3] Sheng-Kai Liao, Wen-Qi Cai, Wei-Yue Liu, Liang Zhang, Yang Li, Ji-Gang Ren, Juan Yin, Qi Shen, Yuan Cao, Zheng-Ping Li, Feng-Zhi Li, Xia-Wei Chen, Li-Hua Sun, Jian-Jun Jia, Jin-Cai Wu, Xiao-Jun Jiang, Jian-Feng Wang, Yong-Mei Huang, Qiang Wang, Yi-Lin Zhou, Lei Deng, Tao Xi, Lu Ma, Tai Hu, Qiang Zhang, Yu-Ao Chen, Nai-Le Liu, Xiang-Bin Wang, Zhen-Cai Zhu, Chao-Yang Lu, Rong Shu, Cheng-Zhi Peng, Jian-Yu Wang, and Jian-Wei Pan. Satellite-to-ground quantum key distribution. *Nature*, 549(7670):43–47, 2017.
- [4] Stephanie Wehner, David Elkouss, and Ronald Hanson. Quantum internet: A vision for the road ahead. *Science*, 362(6412), 2018.
- [5] Gershon Kurizki, Patrice Bertet, Yuimaru Kubo, Klaus MÅymler, David Petrosyan, Peter Rabl, and JÅurġ Schmiedmayer. Quantum technologies with hybrid systems. *Proceedings of the National Academy of Sciences*, 112(13):3866–3873, Mar 2015.
- [6] Stephan Gulde, Mark Riebe, Gavin PT Lancaster, Christoph Becher, JÅurġen Eschner, Hartmut HÅffner, Ferdinand Schmidt-Kaler, Isaac L Chuang, and Rainer Blatt. Implementation of the deutsch–jozsa algorithm on an ion-trap quantum computer. *Nature*, 421(6918):48–50, 2003.
- [7] John Preskill. Quantum computing in the nisq era and beyond. *Quantum*, 2:79, Aug 2018.
- [8] Juan Ignacio Cirac and Peter Zoller. A scalable quantum computer with ions in an array of microtraps. *Nature*, 404(6778):579–581, 2000.
- [9] Sungkun Hong, Michael S Grinolds, Linh M Pham, David Le Sage, Lan Luan, Ronald L Walsworth, and Amir Yacoby. Nanoscale magnetometry with nv centers in diamond. *MRS bulletin*, 38(2):155, 2013.
- [10] Rolf Simon Schoenfeld and Wolfgang Harneit. Real time magnetic field sensing and imaging using a single spin in diamond. *Physical review letters*, 106(3):030802, 2011.
- [11] Liam T Hall, Jared H Cole, Charles D Hill, and Lloyd CL Hollenberg. Sensing of fluctuating nanoscale magnetic fields using nitrogen-vacancy centers in diamond. *Physical review letters*, 103(22):220802, 2009.
- [12] Markus Aspelmeyer, Thomas Jennewein, Martin Pfenigbauer, Walter R Leeb, and Anton Zeilinger. Long-distance quantum communication with entangled photons using satellites. *IEEE Journal of Selected Topics in Quantum Electronics*, 9(6):1541–1551, 2003.
- [13] Juan Yin, Yuan Cao, Yu-Huai Li, Sheng-Kai Liao, Liang Zhang, Ji-Gang Ren, Wen-Qi Cai, Wei-Yue Liu, Bo Li, Hui Dai, et al. Satellite-based entanglement distribution over 1200 kilometers. *Science*, 356(6343):1140–1144, 2017.
- [14] Jun Liu, Isaac Nape, Qainke Wang, Adam Vallés, Jian Wang, and Andrew Forbes. Multidimensional entanglement transport through single-mode fiber. *Science Advances*, 6(4), 2020.
- [15] Daniele Cozzolino, Davide Bacco, Beatrice Da Lio, Kasper Ingerslev, Yunhong Ding, Kjeld Dalgaard, Poul Kristensen, Michael Galili, Karsten Rottwitt, Siddharth Ramachandran, et al. Orbital angular momentum states enabling fiber-based high-dimensional quantum communication. *Physical Review Applied*, 11(6):064058, 2019.
- [16] Georgios M Nikolopoulos, Igor Jex, et al. *Quantum State Transfer and Network Engineering*. Springer, 2014.
- [17] M. Christandl, N. Datta, A. Ekert, and A. J. Landahl. Perfect state transfer in quantum spin networks. *Phys. Rev. Lett.*, 92(18):187902, May 2004.
- [18] G. M. Nikolopoulos, D. Petrosyan, and P. Lambropoulos. Electron wavepacket propagation in a chain of coupled quantum dots. *J. Phys. Condens. Matter*, 16(28):4991, Jul 2004.
- [19] Yaoxiong Wang, Feng Shuang, and Herschel Rabitz. All possible coupling schemes in xy spin chains for perfect state transfer. *Physical Review A*, 84(1):012307, 2011.
- [20] P. Karbach and J. Stolze. Spin chains as perfect quantum state mirrors. *Phys. Rev. A*, 72(3):030301, Sep 2005.
- [21] L. Vinet and A. Zhedanov. How to construct the spin chains with perfect state transfer. *Phys. Rev. A*, 85(1):012323, Jan 2012.
- [22] Marta P. Estarellas, Irene D’Amico, and Timothy P. Spiller. Topologically protected localised states in spin chains. *Scientific Reports*, 7:42904, Feb 2017.
- [23] Andrea Blanco-Redondo, Imanol Andonegui, Matthew J. Collins, Gal Harari, Yaakov Lumer, Mikael C. Rechtsman, Benjamin J. Eggleton, and Mordechai Segev. Topological optical waveguiding in silicon and the transition between topological and trivial defect states. *Phys. Rev. Lett.*, 116:163901, 2016.
- [24] Stefano Longhi. Topological pumping of edge states via adiabatic passage. *Phys. Rev. B*, 99:155150, Apr 2019.
- [25] I. D’Amico, B. W. Lovett, and T. P. Spiller. Freezing distributed entanglement in spin chains. *Phys. Rev. A*, 76(3):030302, Sep 2007.
- [26] T. P. Spiller, I. D’Amico, and B. W. Lovett. Entanglement distribution for a practical quantum-dot-based quantum processor architecture. *New J. Phys.*, 9(1):20, Jan 2007.
- [27] Marta P Estarellas, Irene D’Amico, and Timothy P Spiller. Robust quantum entanglement generation and generation-plus-storage protocols with spin chains. *Phys. Rev. A*, 95(4):042335, 2017.
- [28] Tony J. G. Apollaro, Guilherme M. A. Almeida, Salvatore Lorenzo, Alessandro Ferraro, and Simone Paganelli. Spin chains for two-qubit teleportation. *Phys. Rev. A*, 100:052308, Nov 2019.
- [29] R Ronke, I D’Amico, and TP Spiller. Knitting distributed cluster-state ladders with spin chains. *Physical Review A*, 84(3):032308, 2011.
- [30] Yaroslav Tserkovnyak and Daniel Loss. Universal quantum computation with ordered spin-chain networks. *Physical Review A*, 84(3):032333, 2011.
- [31] Andrew Landahl, Matthias Christandl, Nilanjana Datta, and Artur Ekert. Information processing in quantum spin systems. In *AIP Conference Proceedings*, volume 734, pages 215–218. American Institute of Physics, 2004.
- [32] Agoston E Eiben and Jim Smith. From evolutionary computation to the evolution of things. *Nature*,

- 521(7553):476–482, 2015.
- [33] Agoston E Eiben, James E Smith, et al. *Introduction to evolutionary computing*. Springer.
- [34] Gregory Hornby, Al Globus, Derek Linden, and Jason Lohn. Automated antenna design with evolutionary algorithms. In *Space 2006*, page 7242. 2006.
- [35] B Evans and SP Walton. Aerodynamic optimisation of a hypersonic reentry vehicle based on solution of the boltzmann–bgk equation and evolutionary optimisation. *Applied Mathematical Modelling*, 52:215–240, 2017.
- [36] Xin Yao. Evolving artificial neural networks. *Proceedings of the IEEE*, 87(9):1423–1447, 1999.
- [37] Michael Schmidt and Hod Lipson. Distilling free-form natural laws from experimental data. *Science*, 324(5923):81–85, 2009.
- [38] Darrell Whitley. A genetic algorithm tutorial. *Statistics and computing*, 4(2):65–85, 1994.
- [39] H Moon, DT Lennon, J Kirkpatrick, NM van Esbroeck, LC Camenzind, Liuqi Yu, F Vigneau, DM Zumbühl, G Andrew D Briggs, MA Osborne, et al. Machine learning enables completely automatic tuning of a quantum device faster than human experts. *arXiv preprint arXiv:2001.02589*, 2020.
- [40] NM van Esbroeck, DT Lennon, H Moon, V Nguyen, F Vigneau, LC Camenzind, L Yu, DM Zumbühl, GAD Briggs, Dino Sejdinovic, et al. Quantum device fine-tuning using unsupervised embedding learning. *arXiv preprint arXiv:2001.04409*, 2020.
- [41] R Ronke, TP Spiller, and I D’Amico. Effect of perturbations on information transfer in spin chains. *Physical Review A*, 83(1):012325, 2011.
- [42] Scott M Thede. An introduction to genetic algorithms. *Journal of Computing Sciences in Colleges*, 20(1):115–123, 2004.
- [43] Julian Struck, Christoph Ölschläger, R Le Targat, Parvis Soltan-Panahi, André Eckardt, Maciej Lewenstein, Patrick Windpassinger, and Klaus Sengstock. Quantum simulation of frustrated classical magnetism in triangular optical lattices. *Science*, 333(6045):996–999, 2011.
- [44] See Supplemental Material at [URL will be inserted by publisher] for additional examples of algorithm scaling, examples of optimization processes, and visualization of the genome.
- [45] S. Bose. Quantum communication through an unmodulated spin chain. *Phys. Rev. Lett.*, 91(20):207901, Nov 2003.
- [46] S. Bose. Quantum communication through spin chain dynamics: an introductory overview. *Contemp. Phys.*, 48(1):13, Jan 2007.
- [47] M. Christandl, N. Datta, T. C. Dorlas, A. Ekert, A. Kay, and A. J. Landahl. Perfect transfer of arbitrary states in quantum spin networks. *Phys. Rev. A*, 71(3, Part A):032312, Mar 2005.
- [48] A. Kay. *Int. J. Quantum Inf.*, 8:641, 2010.
- [49] D. Burgarth and S. Bose. Conclusive and arbitrarily perfect quantum-state transfer using parallel spin-chain channels. *Phys. Rev. A*, 71(5):052315, May 2005.
- [50] T. J. Osborne and N. Linden. Propagation of quantum information through a spin system. *Phys. Rev. A*, 69(5):052315, May 2004.
- [51] V. Kostak, G. M. Nikolopoulos, and I. Jex. Perfect state transfer in networks of arbitrary topology and coupling configuration. *Phys. Rev. A*, 75(4):042319, Apr 2007.